

# TBM Performance Analysis in Pyroclastic Rocks: A Case History of Karaj Water Conveyance Tunnel

J. Hassanpour · J. Rostami · Mashalah Khamsehchiyan ·  
A. Bruland · H. R. Tavakoli

Received: 21 June 2008 / Accepted: 22 July 2009 / Published online: 6 August 2009  
© Springer-Verlag 2009

**Abstract** Karaj Water Conveyance Tunnel (KWCT) is 30-km long and has been designed for transferring 16 m<sup>3</sup>/s of water from Amir-Kabir dam to northwest of Tehran. Lot No. 1 of this long tunnel, with a length of 16 km, is under construction with a double shield TBM and currently about 8.7 km of the tunnel has been excavated/lined. This paper will offer an overview of the project, concentrating on the TBM operation and will review the results of field performance of the machine. In addition to analysis of the available data including geological and geotechnical information and machine operational parameters, actual penetration and advance rates will be compared to the estimated machine performance using prediction models, such as CSM, NTNU and  $Q_{TBM}$ . Also, results of analysis to correlate TBM performance parameters to rock mass characteristics will be discussed. This involves statistical analysis of the available data to develop new empirical methods. The preliminary results of this study revealed that the available prediction models need some corrections or

modifications to produce a more accurate prediction in geological conditions of this particular project.

**Keywords** Rate of penetration · Field penetration index · TBM performance · Boreability

## 1 Introduction

Performance of a TBM in a given project depends on many factors which can be classified in 3 categories: (1) Machine specifications, (2) Ground characteristics and (3) Operating parameters. In tunneling projects, ground characteristics or boreability of the rock mass is an important parameter for selecting machine type and specifications. It is clear that proper evaluation of rock mass boreability can also play a major role in machine operation to achieve the best performance. Boreability is the term commonly used to express the ease or difficulty of rock mass excavation by a tunnel boring machine. There are several methods (prediction models) developed by researchers to determine boreability of rock masses and its relation to machine performance (e.g. Blindheim 1979; Rostami and Ozdemir 1993; Rostami 1997; Bruland 1998; Barton 2000).

On the other hand, growth of TBM manufacturing technology and existence of some shortcomings in the prediction models have made it necessary to perform more research on the adjustment of the models for application in special cases. Recently, many researchers have worked on development of new TBM performance prediction models or modification and adjustment of existing models. Ribacchi and Lembo-Fazio (2005) evaluated the relationship between RMR and performance of a double shield machine in the Varzo tunnel. Also Sapigni et al. (2002) studied the empirical relation between RMR and penetration rate.

---

J. Hassanpour · M. Khamsehchiyan (✉)  
Department of Engineering Geology,  
Tarbiat Modares University, Tehran, Iran  
e-mail: Khamechm@modares.ac.ir

J. Rostami  
Department of Energy and Mineral Engineering,  
Pennsylvania State University, University Park, PA, USA

A. Bruland  
Department of Civil and Transportation Engineering,  
Norwegian University of Science and Technology (NTNU),  
Trondheim, Norway

H. R. Tavakoli  
SCE Company, Tehran, Iran

Cassinelli et al. (1982) used correlation between rock structure rating system (RSR) and actual TBM performance to evaluate the penetration rate.

Sanio (1985) found strong correlations between uniaxial compressive strength (UCS) of rock and the specific energy defined as the amount of energy needed to excavate a unit volume of rock. Bruland (1998) updated and improved the NTNU model (introduced by Blindheim 1979) based on field data mainly collected from Norwegian tunnels. Rostami and Ozdemir (1993) and Rostami (1997) developed the CSM model for cutting force estimation of disc cutters based on the Brazilian tensile strength (BTS) and UCS of rock. Subsequently, Yagiz (2002) modified the CSM model adding rock mass properties as an input parameter into the model. Ramezanzadeh et al. (2008) has also followed up on this work and developed a database of TBM field performance for over 60 km of tunnels. Then, he offered adjustment factors for CSM models to account for joints and discontinuities.

Barton (1999, 2000) reviewed a wide range of TBM tunnels to establish the database for estimating penetration and advance rate. Yagiz (2007) has also performed statistical analysis on data obtained from Queens's tunnel (New York) and proposed an empirical model to predict TBM penetration rate. He has related four rock mass parameters (UCS, Punch test index or PSI, spacing and orientation of joints) to penetration rate of machine. In a similar research work, Gong and Zhao (2009) by performing a nonlinear regression analysis on data obtained from two tunnels excavated in granitic rock masses in Singapore, developed an empirical equation to estimate boreability of rock mass. They proposed a relationship between four rock mass parameters (UCS, brittleness, joint count number and orientation of joints) and boreability index of the rock mass.

In this research, actual data obtained from the bored section of the KWCT project was used to compare the results of the prediction models with actual boreability of the rock mass and actual machine performance in an attempt to evaluate accuracy of each model. In this study, effects of geological parameters on machine performance in the Pyroclastic rocks of the Karaj formation have also been evaluated.

## 2 Project Description

The Karaj Water Conveyance Tunnel has been designed to transfer  $16 \text{ m}^3/\text{s}$  of water from the Karaj (Amir-Kabir) Dam northeast of Karaj City to Tehran City (Fig. 1). The tunnel was divided into two sections: Lot 1 or ET-K (16 km) at the southeast end and Lot 2 or K-P (14 km) at the northwest end of the project area. Currently, the ET-K section is under construction from a portal at the southeast

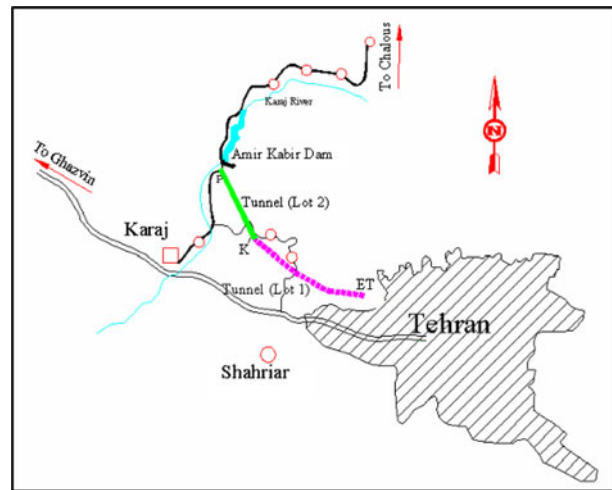


**Fig. 1** Details of Karaj water conveyance tunnel scheme, northwest of Tehran

end of the tunnel. The northwestern section will be built from a 25-m deep shaft known as Shaft K.

At the ET portal, a double shield TBM was launched from a 159 m starting tunnel excavated by drill and blast method. The tunnel is lined with pre-cast concrete segments with tetragonal arrangement and thickness of 25 cm.

The elevation of K and ET points at the two ends of the section are 1,582 m and 1,564.4 m MSL, respectively, obtaining a slope of 0.013% toward the southeast portal. The maximum rock cover in the ET-K section is about 600 m, with an average of about 400 m.

## 3 Geology of the Project Area

In the preliminary studies (SCE Company 2006), main geological, engineering geological and hydrogeological characteristics of the tunnel along the alignment were described as follows:

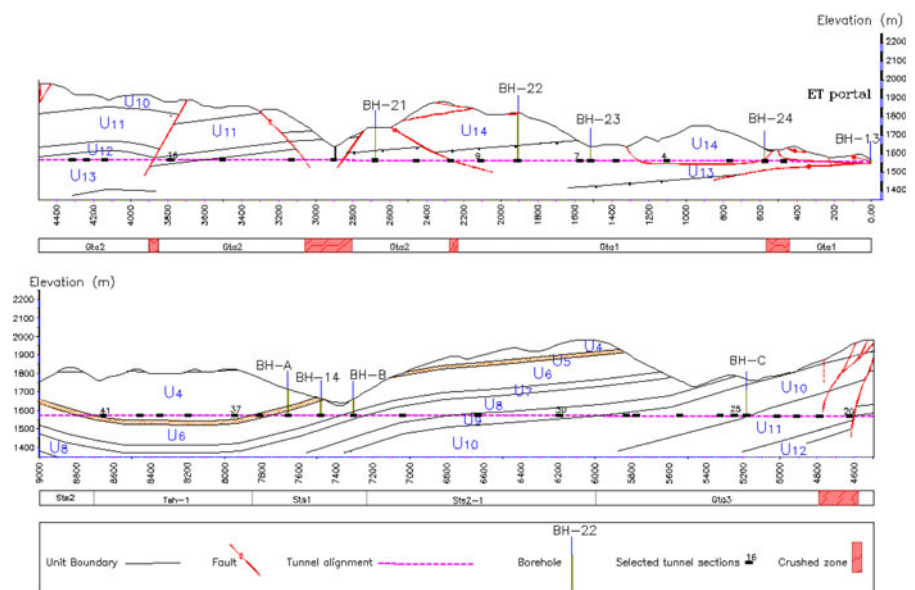
### 3.1 Stratigraphy

The main geological unit outcropped in the project area is the Karaj formation, a well-known formation of the Alborz Mountains. The formation is composed of a variety of pyroclastic rocks, often interbedded with sedimentary rocks. The characteristic rock type is a green vitric to crystal lithic tuff, but other tuffs, such as tuff breccias, and sandy and silty tuffs occur together with shales, siltstones and sandstones.

During the geological studies in the project area, 14 predominant stratigraphic units were identified along the tunnel alignment. Table 1 lists 11 stratigraphic units encountered in the bored section of the tunnel. These units are different members of the Karaj formation. The

**Table 1** Stratigraphic and engineering geological units identified along the tunnel

No.	Stratigraphic units	Lithology	Engineering geological units	Description
1	U14	Undifferentiated rocks of U11 to U13 units	Gta1	Weak to moderately strong, thin to moderately bedded, intensely fractured, may be unstable
2	U13	Sandstone, green vitric tuff and siliceous tuff	Gta2	Weak to moderately strong, thin to moderately bedded, moderately fractured, may be unstable
3	U12	Light cream lithic and vitric tuff		
4	U11	Sandstone and micro-conglomerate	Gta3	Moderately strong to strong, moderately to thick bedded, slightly fractured, stable
5	U10	Siliceous green tuff and sandstone		
6	U9	Green vitric and lithic tuff and siltstone	Sts2	Very strong, thick bedded, stable
7	U8	Siliceous green tuff and sandstone		
8	U7	Massive green tuff	Sts1	Weak to moderately strong, thin to moderately bedded, fractured, may be unstable
9	U6	Tuffaceous siltstone		
10	U5	Sandstone and micro-conglomerate		
11	U4	Alternation of thin bedded shale, siltstone and sandstone	Tsh	Weak to moderately strong, thin to moderately bedded, foliated, fractured, may be unstable
–	–	–	Cz	Weak to moderately strong, intensely fractured, unstable

**Fig. 2** Geological cross section along the tunnel

geological profile of the tunnel in Fig. 2 shows the distribution of these rock units along the bored section of the tunnel.

### 3.2 Structural Geology

The area around the tunnel is moderately folded and intensely faulted. As shown in geological cross section (Fig. 2), the bored section of the tunnel has passed through a wide syncline (Azgilak syncline) and anticline (Vardij anticline) and some thrust faults with different length of

influence zone. Due to folded structure of the area and existence of some thrust faults, the tunnel route can be divided into several structural zones. Orientation of bedding planes and related structures (joint sets) changes in different structural zones.

The most important thrust faults in the area are the Poorkan-Vardij and North Tehran faults. Although the alignment has been chosen to avoid these two major faults, the first 3 km of tunnel have passed through the zone of influence of these two major faults, resulting in many delays due to instabilities in the tunnel walls. In

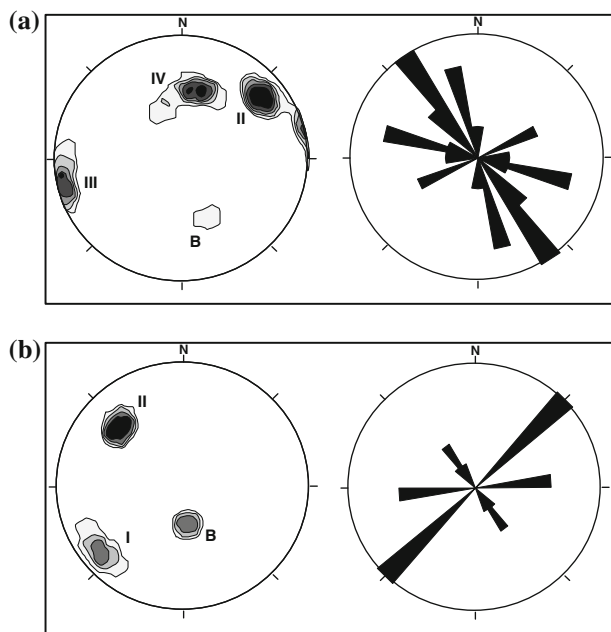


**Fig. 3** Main discontinuity sets measured in surface outcrops at: **a** influence zone of Poorkan-Vardij and North Tehran faults and **b** Vardij anticline near BHA borehole

addition, some minor faults and shear zones have been identified as crossing the tunnel line. The thickness of the fault zones are thought to be generally between 10 and 50 m.

In the first 3 km of tunnel, usually more than 3 joint sets with low values of average spacing can be observed in the tunnel. Further along the tunnel, rock quality changes to less fractured rock mass with less number of joint sets and higher values of average spacing. Normally in most sections of the tunnel there are at least 2 conjugate joint sets in addition to bedding planes. Figure 3a and b show stereographic projection and rose diagrams of main discontinuity sets measured in two surface outcrops in different parts of the tunnel. Comparing the results of tunnel mapping with those of surface joint mapping, reasonable correlations can be observed.

### 3.3 Engineering Geology

The bored section of the tunnel can be subdivided into 7 segments (engineering geological units) with uniform characteristics related to TBM performance, tunnel stability and groundwater inflow. This was based on studies of outcrops, core boxes and also results of laboratory and field tests. General characteristics of identified engineering geological units are listed in Table 1. Average geomechanical characteristics of the engineering geological units in the area were assessed using some empirical rock mass classification systems, such as RQD (Deere et al. 1967), RMR (Bieniawski 1989), GSI (Hoek et al. 1995, Hoek 2007) and Q-system (Barton et al. 1974). Summary results are listed in Table 2.

As shown in Table 2, the rock quality in the completed section of the tunnel is highly variable. In some parts of the tunnel RQD of 100% have been measured, whereas elsewhere crushed tuff with low RQD of less than 25% has been observed. Quality of rock in fault zones is very bad with typical RQD of less than 25%.

In addition to variations of fracturing, a wide range of variations can be observed in intact rock properties, such as density, porosity, UCS and tensile strength. For instance, UCS of rock in different engineering geological units varies from minimum 30 to maximum 160 MPa, depending on lithology and degree of alteration.

### 3.4 Groundwater Condition

Groundwater condition along the tunnel varies from dry to continued flow of water in local confined aquifers. At least 35% of the bored section of the tunnel is constructed above the groundwater table. In the first 3 km of tunnel, no water was encountered but some water inflow was experienced in the remaining parts of the tunnel. The magnitude of the flow was regulated primarily by the permeability of the fracture systems. Nearly all permeability tests performed in the boreholes drilled in different geological units, yielded Lugeon values below 1, indicating very low permeability in

**Table 2** Summary results of the rock mass classification in the project area

Rock type	Average spacing (m)	NTNU class	RQD (%)	Discontinuity condition	GSI	Basic RMR	<i>Q</i>
Gta1	0.1–0.2	III to II	25–50	Poor	20–40	30–50	0.5–2
Gta2	0.2–0.3	II to I–II	40–60	Fair	30–60	45–60	2–15
Gta3	0.3–0.4	I to I–II	60–80	Very good	60–80	60–70	20–50
Sts1	0.3–0.6	I to I–I+	60–90	Good	65–80	55–70	15–30
Sts2	0.6–0.8	I–I– to I–	75–100	Good	70–85	70–80	30–40
Tsh	0.25–0.5	II– to I–(I–)	60–80	Very good	50–75	55–65	15–50
Cz	<0.1	IV to III	<25	Very poor	<20	<30	<0.1

the bedrock. Therefore, anticipated and encountered groundwater flow was very low, except for crushed zones. This means that the groundwater condition along the tunnel is primarily “damp to wet” and infrequently “dripping”. A limited number of local confined aquifers with high water pressures (up to 8 bars) were encountered, but water inflow did not exceed 30 l/s.

#### 4 Tunneling Operation

The site preparation started in 2004 and the TBM arrived at the site in May 2006. TBM assembly was accomplished in 15 weeks and mining commenced in August 2006. At the date of preparing this paper (January 2008), some 8,700 m of tunnel was completed.

The double shield TBM procured for this project was manufactured by Herrenknecht. The cutterhead (Fig. 4) is laced with 31, each 17 inch or 432 mm diameter disc cutters with a load capacity of 250 kN. Other main technical data for the TBM are summarized in Table 3.

The weekly average performance parameters are shown in Fig. 5. As shown in graph (a) of Fig. 5 about 8.7 km of tunnel was completed in 74 full working weeks or about 500 working days at an average rate of about 115 m/week. Weekly average of penetration rate ranges between 2 and 5.3 m/h with an average of 3.62 m/h (Fig. 5b). Maximum and average weekly utilization factor was 30.3 and 19.1%, respectively (Fig. 5d).

Also results of analysis of daily performance of the machine show that maximum TBM advance of 38.9 m/day, rate of penetration of 6.3 m/h and utilization factor of 42% were experienced during this time, however, not all on the same date.

Figure 6 shows average time distribution of different activities in the tunnel for the first 8.7 km of tunnel from



**Fig. 4** Double shield TBM at the ET portal

**Table 3** Main specifications of TBM

Parameter	Value
Machine diameter	4.65 m
Cutters diameter	432 mm
Number of disc cutters	31
Disc nominal spacing	90 mm
Maximum operating cutterhead thrust	16,913 kN
Cutterhead power	$5 \times 250 = 1,250$ kW
Cutterhead speed	0 to 11 rpm
Cutterhead torque (nominal)	1,723 kNm (6.58 rpm)
	1,029 kNm (11 rpm)
Thrust cylinder stroke	1,400 mm
Conveyor capacity (approx.)	200 m <sup>3</sup> /h
TBM weight (approx.)	170 tons

August 2006 to January 2008. As shown, advance time which includes required times for boring, segment installation and re-gripping comprises 26% of all activities. In the bored section of the tunnel, the main downtime in TBM advance included times required for repairing of different parts of the TBM and back-up system (31%), delays due to adverse geological conditions (14%) and delays related to site management and logistics (13%). Routine maintenance and shift change were also a part of downtime that influenced the TBM utilization and accounted for 16% of total time.

Most important adverse geological conditions that have caused delays in the TBM advance include:

- Collapse of tunnel face and jamming of the cutter head in crushed zones.
- Groundwater inflow and related difficulties for tunneling.
- Increasing of cohesive fine grained particles in muck and additional time to clean disc cutters for maintenance.
- Increasing disc cutter changes due to mixed face condition in some tunnel sections.

#### 5 TBM Field Performance Database

One of the main objectives of this study was to develop a database of TBM performance to compile collected field data for further analyses. For this purpose, results of studies performed during the pre-construction phase and construction phase have been combined in a database.

A detailed study of geology, engineering geology and hydrogeology of the project area has been performed in a scale of 1:2,000 during the pre-construction phase (SCE Company 2006). Also, a total of 15 borings were



**Fig. 5** Weekly average of TBM performance parameters: **a** TBM advance, **b** rate of penetration, **c** advance rate and **d** utilization factor

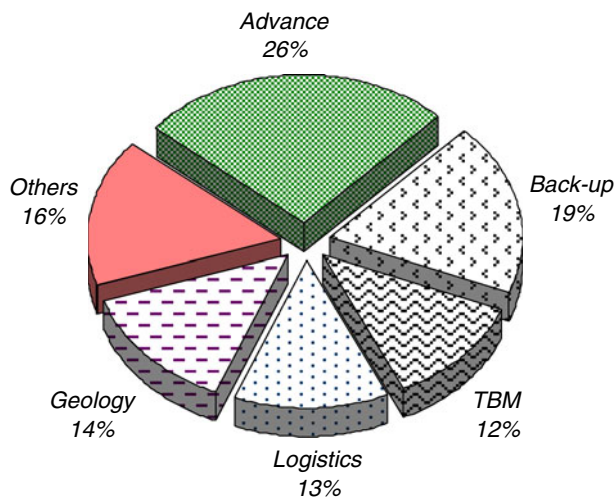
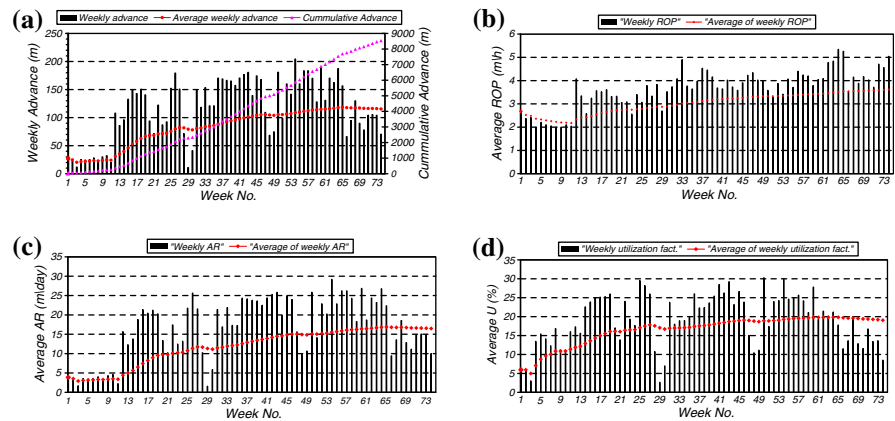


**Fig. 6** Average tunneling time consumption in the bored section of the tunnel

completed along the tunnel alignment to obtain core samples. Among drilled boreholes, 10 boreholes were located in the bored section of the tunnel and have been used for characterizing and analyzing boreability of the rock mass for this study. Many samples were taken from boreholes to perform required tests for determination of physical, mechanical and drillability characteristics of the different rock units.

During the construction phase and through back mapping of the tunnel, information, such as rock type, rock mass fracturing, joint condition, characteristics of fault zones, rock durability information, weathering/alteration characteristics, groundwater and rock stability information were recorded on mapping sheets. Data obtained from the back mapping of the tunnel was used to analyze TBM performance and also to verify design assumptions. In addition, machine performance data and operating parameters (such as applied thrust, RPM, torque, etc.) were recorded continuously by data acquisition system. During

back mapping, many samples were taken from the muck to perform tests, such as point load index test and petrographic analysis.

Developed database consists of three main sections. The first section includes some parameters like net boring time and length of mined section and also the average of machine operational parameters (thrust, RPM, power and applied torque) through the section length. These parameters were obtained from the daily operating records and the TBM data logger. In the second section, results of ground characterization (laboratory and field measured parameters) are listed. In Sect. 3, penetration rate in different reaches of the tunnel has been calculated (based on data arranged in sections 1 and 2, and using some existing prediction models).

## 6 TBM Performance Modeling

The prediction of TBM performance refers to the estimation of rate of penetration (ROP), machine utilization (U) and advance rate (AR). A wide variety of performance prediction methods have been offered and are being used in different projects. In general, most commonly used TBM performance prediction models are:

1. Theoretical/experimental models (based on laboratory full scale cutting testing and cutting forces);
2. Empirical methods (based on field performance of TBMs and some rock properties).

In this research, the CSM model (Rostami 1997) of the first group and the NTNU (Bruland 1998) and  $Q_{TBM}$  (Barton 2000) models of the second group were used to analyze TBM performance. The most important output parameter in these models is the rate of penetration (ROP). Each model needs different input parameters to estimate ROP. Required input parameters for the above mentioned models are listed in Table 4.

**Table 4** Input parameters in applied prediction models

Prediction model	Required input parameters	
	Rock mass parameters	Machine parameters
NTNU (Bruland 1998)	Fracturing: frequency and orientation, drilling rate index (DRI), bit wear index (BWI) and cutter life index (CLI), porosity, and other parameters	Cutter thrust, cutter spacing, cutter diameter
CSM (Rostami and Ozdemir 1993)	Unconfined compressive strength (UCS), Brazilian tensile strength (BTS) and Cerchar abrasivity index (CAI)	Cutter load capacity, cutter spacing, cutter diameter, cutter tip width, and TBM thrust and torque
$Q_{TBM}$ (Barton 2000)	$RQD_0$ , $J_n$ , $J_r$ , $J_a$ , $J_w$ , SRF, rock mass strength, cutter life index (CLI), UCS, induced biaxial stress	Average cutter load, TBM diameter

## 7 Post Construction Geological Investigations

To characterize the ground along the tunnel, two sets of parameters, including intact rock properties and rock mass characteristics have been estimated or measured by tunnel face observation, reviewing core samples and performing laboratory tests on samples taken from the boreholes and the muck.

This tunnel was excavated by a shielded machine and lined with precast segmental lining. Consequently, there were some limitations to the mapping of the geological features. An attempt was made in this research to select parts of the tunnel, where sufficient and reliable geological data were available. Available data were collected from the following general locations within the tunnel:

- A borehole extending to the tunnel level was in the general area.
- Rock face observed and investigated during geological back mapping.
- Extrapolation of surface geological parameters to the tunnel level, maintaining a high level of reliability due to special geological conditions.

About 40 sections of the bored tunnel have been selected based on the aforementioned criteria. Exact locations of these sections are shown in Fig. 2. These sections have a length of 10–20 m each.

### 7.1 Intact Rock Properties

In general, the TBM performance is partly controlled by intact rock properties, such as petrographic characteristics, physical and mechanical properties and drillability. Each of these rock parameters have been evaluated by laboratory testing.

In addition to physical and mechanical tests performed at design stage, some samples were obtained and tested during the construction phase. Overall, more than 170 samples were taken from boreholes and surface exposures.

The summary results for rock mechanics testing are listed in Table 5.

In Table 5 all rock units are classified into 5 main lithotypes. This classification is based on microscopic characteristics (mineralogy and texture) of the different rock units which were evaluated by studying more than 100 thin sections and can be a suitable tool to simplify characterization of intact rocks. In fact, lithologies described by geologists in the field for the stratigraphic units are summarized in Table 1. A rough estimate of distribution of the identified lithotypes in the bored section of tunnel is shown in Fig. 7.

As shown in Table 5 and box-plots in Fig. 8a and b, the UCS and tensile strength of different lithotypes range from 30 to 160 MPa and 5 to 12 MPa, respectively.

To determine drillability indices of the rock units, two representative samples from borehole BHA and BHC have been tested at SINTEF/NTNU rock laboratories in Trondheim, Norway. These samples have been subject to a complete set of NTNU boreability tests. Results of these tests are listed in Table 6.

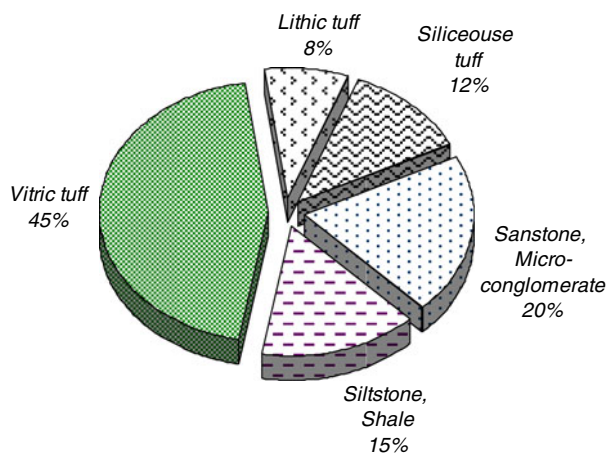
Obviously two tests are insufficient for any meaningful analysis of rock characteristics as related to TBM performance. Therefore, additional boreability indices were estimated from some proposed graphs and tables presented in reports published by the Norwegian University of Science and Technology (Bruland 1998). Table 7 summarizes the results of estimation of drillability indices for different lithotypes along the tunnel.

### 7.2 Rock Mass Characteristics

A rock mass can be massive, fractured or highly fractured depending on the geological and tectonic conditions of the site. When the rock mass is massive, intact rock properties, such as UCS and tensile strength are the most desirable parameters for estimating TBM advance since there is no need to consider weakness planes. Planes of weakness in the rock mass can significantly impact the net penetration

**Table 5** Main characteristics of lithotypes

Lithotype	Percent of lithotypes in geological units	Minerals	Quartz content (%)	Density (g/cm <sup>3</sup> )	Porosity (%)	UCS (MPa)	Tensile strength (MPa)	Number of samples
Vitric tuff	U14 (85%), U13 (80%), U12 (95%), U7 (95%)	Feldspars, clay minerals, calcite, quartz	5	2.3–2.5	1–10	30–100	5–10	67
Lithic tuff	U14 (5%), U12 (5%), U9 (80%), U7 (5%)	Rock fragments, feldspars, clay minerals, chlorite, quartz	15	2.4–2.5	3–6	50–80	6–8	32
Siliceous tuff	U14 (5%), U13 (15%), U10 (50%), U8 (35%)	Silica, feldspars, clay minerals, quartz	30	2.65	1–3	80–160	8–12	26
Sandstone, micro-conglomerate	U14 (5%), U13 (5%), U11 (100%), U10 (50%), U8 (65%), U5 (100%), U4 (10%)	Feldspars, clay minerals, calcite, chlorite, quartz	20	2.4–2.6	1–5	40–80	6–8	32
Siltstone, shale	U9 (20%), U6 (100%), U4 (90%)	Clay minerals, calcite, quartz, chlorite	10	2.4–2.5	1–5	30–50	5–6	14

**Fig. 7** Distribution of main lithotypes identified along the bored section of the tunnel

rate and cutter wear of TBMs. Fractures and joints in the rock mass influence rock boreability depending on their spacing, surface condition and also their orientation with respect to the direction of machine advance.

In the following sections to describe rock mass quality, results of evaluating discontinuities characteristics, classification of rock masses and calculation of rock mass strength parameters in different sections of tunnel will be explained.

### 7.2.1 Characteristics of Discontinuities

The characteristics of the main discontinuity sets in selected sections of tunnel were obtained from measurements and estimations according to ISRM recommendations during back mapping of the tunnel. These characteristics include average joint spacing,  $\alpha$  angle (angle

between critical joint set and tunnel axis), weathering condition and a description of joint surface condition. Figure 9 shows variation of average values of two important discontinuity specifications in selected tunnel sections. As shown, average spacing of discontinuities ranges between 0.1 and 0.8 m. Also variation range of average  $\alpha$  angle is 30–70°.

### 7.2.2 Rock Mass Classification

To investigate the influence of geomechanical parameters on machine performance, it was necessary to have an estimate of classification parameters, such as RQD, RMR,  $Q$ , GSI and NTNU class in each selected section. These parameters are calculated based on average values of intact rock properties, fracturing degree and condition of discontinuities. Results of calculation of different rock mass classification parameters were recorded in Sect. 2 of the database. Figure 10 shows values of three main parameters including basic RMR, GSI and  $Q$  in different tunnel sections. As shown, variations of these parameters through tunnel alignment are very similar to each other.

### 7.2.3 Rock Mass Strength Parameters

Experiences gained from similar research works show that rock mass strength parameters, such as  $Q_c$  (Barton 2000), rock mass compressive strength or  $UCS_{rm}$  (Hoek 2007), rock mass strength or  $\sigma_{cm}$  (Barton 2000) and rock mass cuttability index or RMCI (Bilgin et al. 1997) usually show some correlations with actual machine parameters. The main advantage of the above mentioned parameters is that the effect of intact rock strength and fracturing conditions are included in their formulae as follows:



**Fig. 8** Variation ranges of **a** UCS and **b**  $I_{s50}$  values in different lithotypes

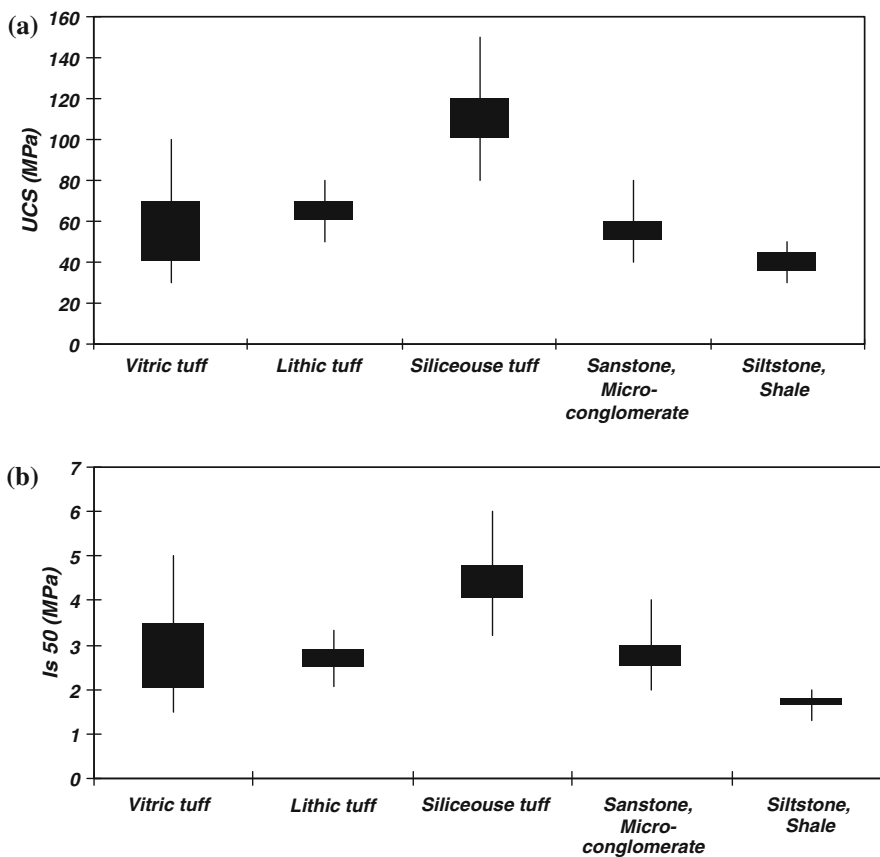


**Table 6** Results of drillability tests

Sample	Lithotype	Brittleness value (S20)	Flakiness	Compaction index
BHC	Vitric tuff	40.7	1.36	0–1
BHA	Sandstone	34.2	1.43	0
Sample	Siever’s J value (Sj)	Abrasion value cutter steel (AVS)	Drilling rate index (DRI)	Cutter life index (CLI)
BHC	81.8	0.5	51	98.4
BHA	85.4	1.0	45	76.6

**Table 7** Estimated values of drillability indices for different lithotypes

Lithotypes	Drilling rate index (DRI)	Cutter life index (CLI)
Vitric tuff	45–55	90–100
Lithic tuff	50–55	75–85
Siliceous tuff	40–45	50–60
Sandstone, micro-conglomerate	45–50	70–80
Siltstone, shale	60–65	70–80

$$RMCI = UCS \left( \frac{RQD}{100} \right)^{2/3} \tag{1}$$

$$Q_c = Q \cdot \frac{UCS}{100} \tag{2}$$

$$\sigma_{cm} = 5 \cdot \gamma \cdot Q_c^{1/3} \tag{3}$$

$$UCS_{rm} = UCS \cdot s^a \tag{4}$$

where

$$s = \exp \left( \frac{100 - GSI}{9 - 3D} \right) \tag{5a}$$

**Fig. 9** Variation of average spacing and  $\alpha$  angle in selected tunnel sections

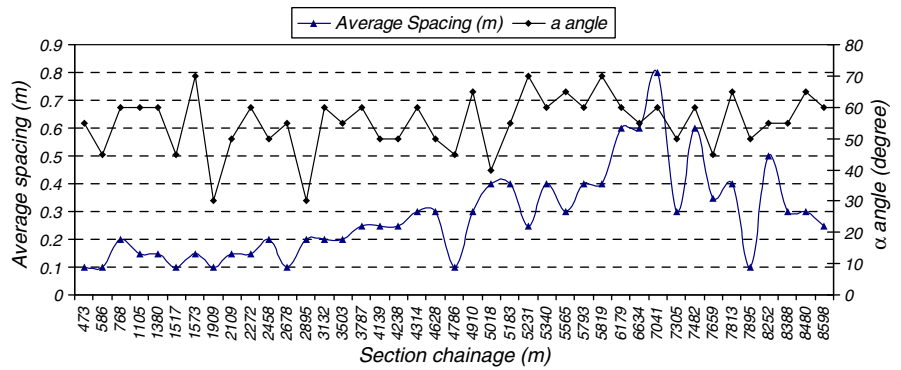


**Fig. 10** Variation of basic RMR, GSI and  $Q$  in selected tunnel sections

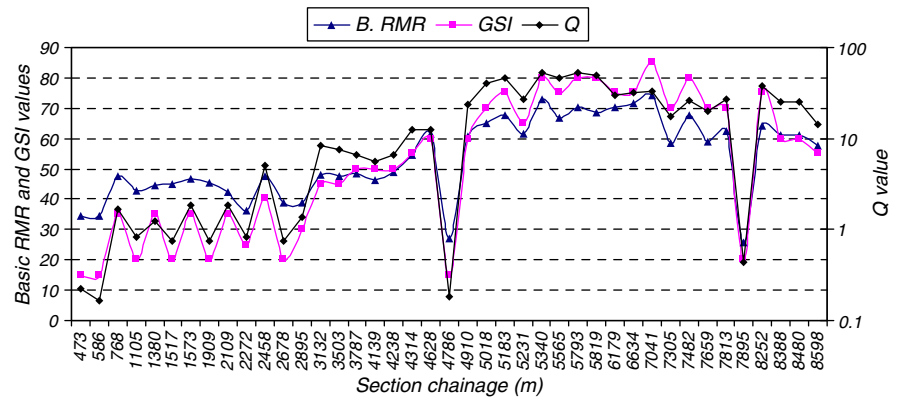
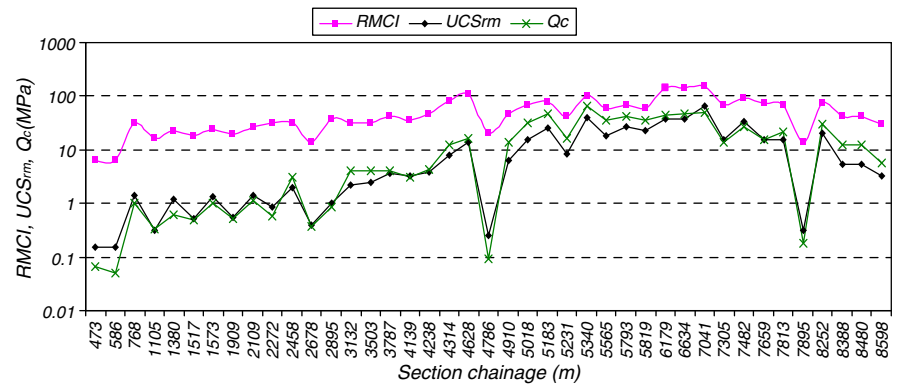


**Fig. 11** Variation of RMCI,  $UCS_{rm}$  and  $Q_c$  in selected tunnel sections



and

$$a = \frac{1}{2} + \frac{1}{6}(e^{-GSI/15} - e^{-20/3}) \tag{5b}$$

In above equations,  $D$  is disturbance factor ( $D = 0$  in TBM projects) and  $\gamma$  is density of rock.

Figure 11 shows values of above mentioned parameters including  $UCS_{rm}$ , RMCI and  $Q_c$  in different tunnel sections.

### 8 TBM Performance in Selected Tunnel Sections

To analyze TBM performance, collected raw data (actual boring time, boring length, maintenance and delays) was

compiled into a spreadsheet (Sect. 1 of the database) and ROP, AR and U for selected tunnel sections were calculated. The most important parameters are average ROP, field penetration index (FPI) and specific energy (SE) which can be calculated using the following formulae:

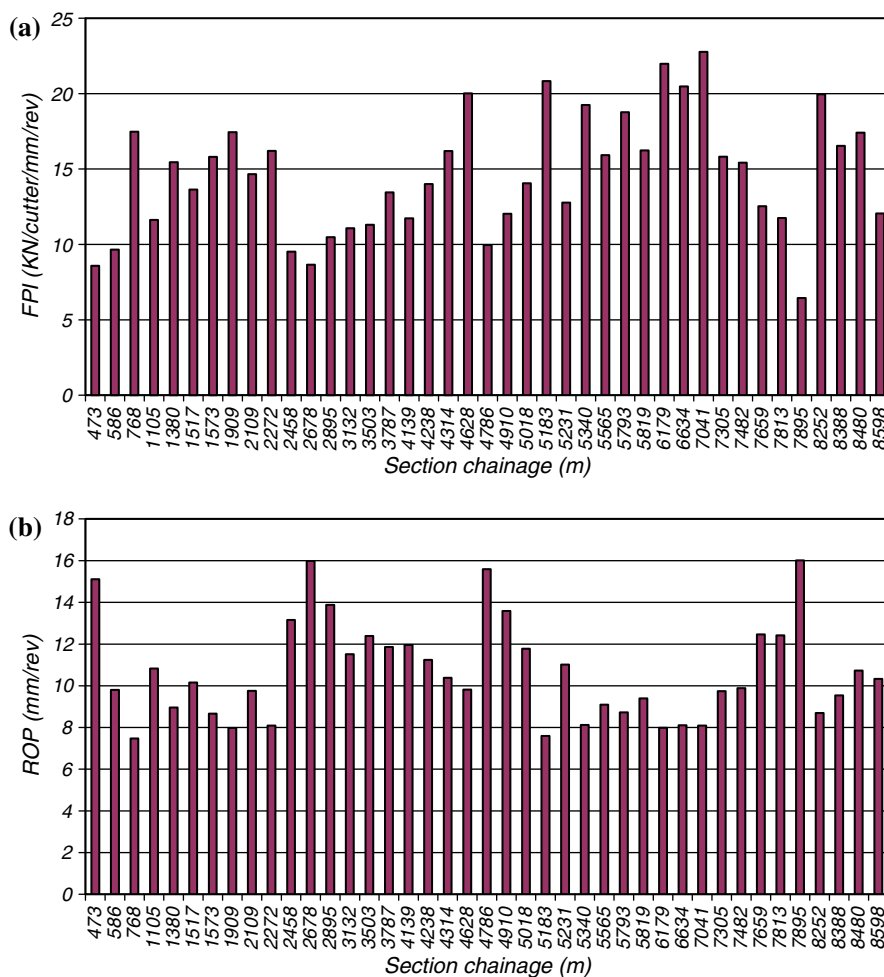
$$ROP(m/h) = \frac{\text{Boring length (m)}}{\text{Boring time (h)}} \tag{6}$$

$$ROP \text{ (mm/rev)} = \frac{ROP \text{ (m/h)} \times 1000}{RPM \times 60} \tag{7}$$

$$FPI = \frac{F_n}{ROP \text{ (mm/rev)}} \tag{8}$$

$$SE = \frac{200 \times N_{TBM} \times r_{mc}}{3 \times d_{TBM}} \times \frac{F_r}{ROP \text{ (mm/rev)}} \tag{9}$$

**Fig. 12** Average field penetration index (a) and actual rate of penetration (b) in selected sections



In the above equations, RPM is cutterhead revolutions (rev/min),  $F_n$  is cutter load or normal force,  $F_r$  is cutter rolling force, ROP is rate of penetration (m/h) or (mm/rev),  $d_{TBM}$  is TBM diameter (m),  $N_{TBM}$  is number of cutters on the cutterhead, SE is specific energy ( $MJ/m^3$ ),  $r_{mc}$  is the weighted average cutter distance from center of rotation (m) and FPI is field penetration index (kN/cutter/mm/rev).

Figure 12a and b show variations of actual FPI and ROP in different sections along the tunnel. As shown, the average ROP and FPI in selected sections generally ranged from 7 to 16 mm/rev and 8 to 23 kN/mm/rev, respectively.

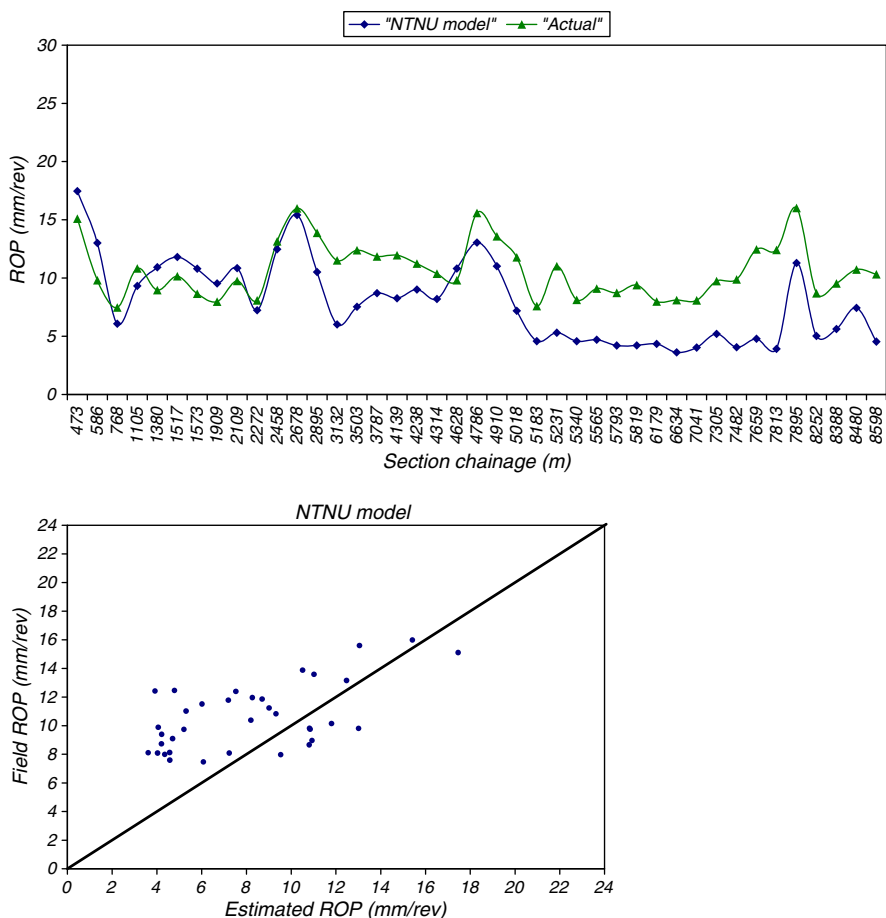
### 9 TBM Performance Predictions

To evaluate the accuracy of the prediction models, it was necessary to apply actual geological and machine operational information as input data to the models and compare the results with actual machine performance. In this research, recorded machine parameters (Sect. 1 of the database) and collected geological data (Sect. 2 of the

database) at each selected tunnel section were used as input data to the CSM, NTNU and  $Q_{TBM}$  models. Estimated penetration rates have been compared with average field penetration rates in each selected tunnel section. Figures 13, 14, 15 show results of this comparison, illustrated in two types of graphs. The following observations can be made from these graphs:

- In general for all three models, the values of estimated ROP are less than actual ROP.
- As shown,  $\Delta ROP$  or difference between predicted penetration rates by various models and the actual penetration rates are very large, exceeding 100% in some tunnel sections.
- Among these three models, the NTNU model shows more reasonable values in comparison to the CSM and  $Q_{TBM}$  model.
- Variation of estimated ROP using the models of NTNU and  $Q_{TBM}$  is more similar to the actual variation of ROP than using the CSM model in selected tunnel sections.

**Fig. 13** Comparison of penetration rate calculated using the NTNU model with actual penetration rate



- ROP values estimated by the original CSM model are sensitive only to intact rock properties and the effect of joints is not included in the model. So, where the intact rock strength is low while the rock mass is blocky or massive, or where the intact rock is very strong, but the rock mass is fractured to intensely fractured, the estimated values of ROP are far from actual values. This can be overcome by the application of recently introduced adjustment factors (Yagiz 2002 and Ramzanzadeh 2005).

**10 Influence of Engineering Rock Properties on TBM Performance**

To investigate the influence of engineering rock properties on TBM performance, first, the correlation between actual ROP and simple parameters like UCS and discontinuity spacing were assessed. Then more complex parameters (e.g. a combination of different parameters) were introduced in the analyses.

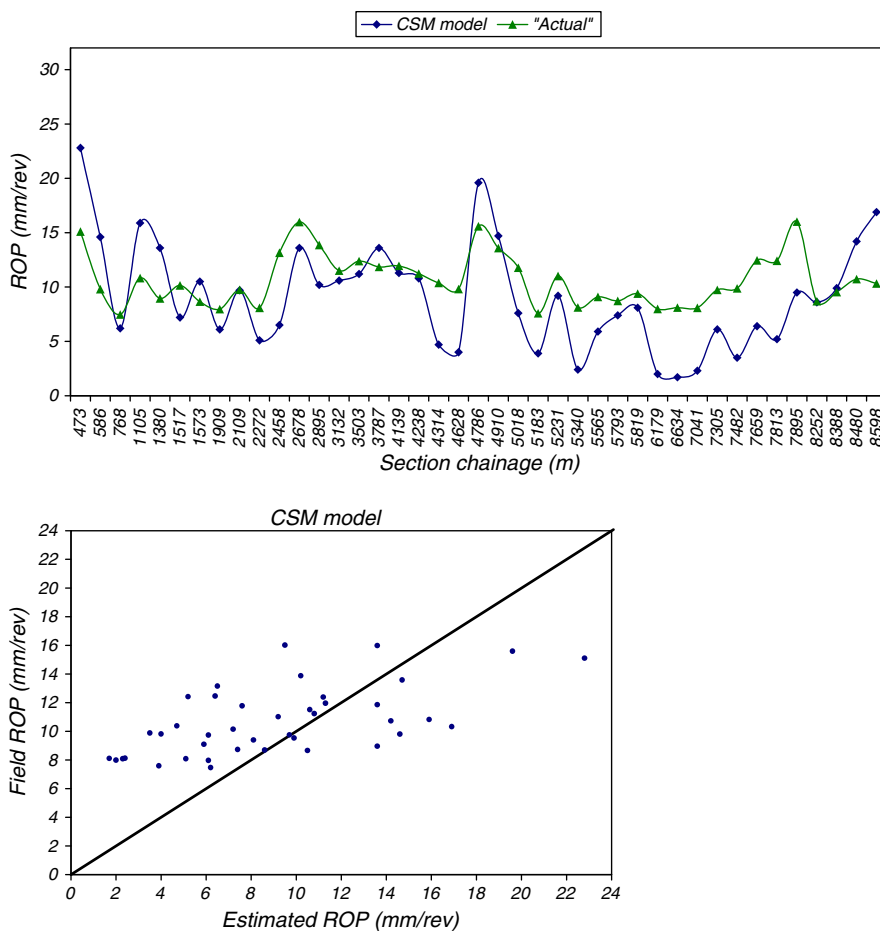
**10.1 Intact Rock Strength**

It is generally believed that among the intact rock properties, UCS provides the most useful indication of machine performance. In some cases, UCS values correlate significantly with TBM performance parameters and have been incorporated into boreability equations. Graphs (a) to (d) of Fig. 16 show the correlation between UCS and machine parameters ROP, SE and FPI. As shown, among the selected machine performance parameters, the field penetration index (FPI) which is a composite parameter shows a better correlation with UCS. Some correlations were also observed between FPI and other geological parameters, however, to lesser extent. Therefore, in this study, FPI was selected as a suitable machine parameter for developing empirical relationships with geological parameters.

**10.2 Joint Frequency**

Spacing and RQD are two commonly used parameters used for describing joint frequency. Correlations between these two parameters with FPI are shown in Fig. 17a and b,

**Fig. 14** Comparison of penetration rate calculated using the CSM model with actual penetration rate



respectively. Although the correlations are quite similar, spacing shows a better correlation with FPI than RQD.

### 10.3 Joint Orientation

Theoretically, orientation of discontinuities (bedding and joint planes) can play a significant role in the TBM boring process. Angle  $\alpha$  which is defined as the smallest angle between the tunnel axis and the discontinuity surface can be a good parameter to evaluate influence of joint/bedding orientation on TBM performance.

On the other hand, experiences gained from similar studies revealed that finding a reasonable relationship between discontinuity orientation alone and TBM parameters is not easy (Ramezanzadeh 2005). In blocky and layered rock masses with two or three similar joint sets perpendicular to bedding planes, the effect of joint orientation can be neglected. It seems that the orientation of discontinuities can affect the boreability and TBM performance most significantly in rock masses with one main discontinuity set (such as thin bedded, foliated and schistose rock masses).

Figure 18 shows the plot of average discontinuity orientation in each selected tunnel section versus average FPI at that section. As can be seen in this graph, only a weak correlation between these two parameters has been obtained.

### 10.4 Rock Mass Quality

In this study, the relationship between different rock mass classification systems (Q-system, basic RMR,  $RMR'_{89}$  and GSI) and actual machine performance (FPI) have been investigated. Graphs (a) to (d) of Fig. 19 show the results of correlating FPI and rock mass classifications.

As shown, basic RMR shows better correlation than  $RMR'_{89}$ . Basic RMR is obtained from the sum of ratings of 5 parameters (UCS, RQD, spacing, joint surface condition and groundwater condition) with no correction factor related to joint orientation.  $RMR'_{89}$  is defined by partial rating relative to water condition as a fixed value ( $R_{Gw} = 15$ ). So, it is observed that although theoretically, water condition is not an effective parameter on penetration rate, it has had a fairly important role on



**Fig. 15** Comparison of penetration rate calculated using the  $Q_{TBM}$  model with actual penetration rate

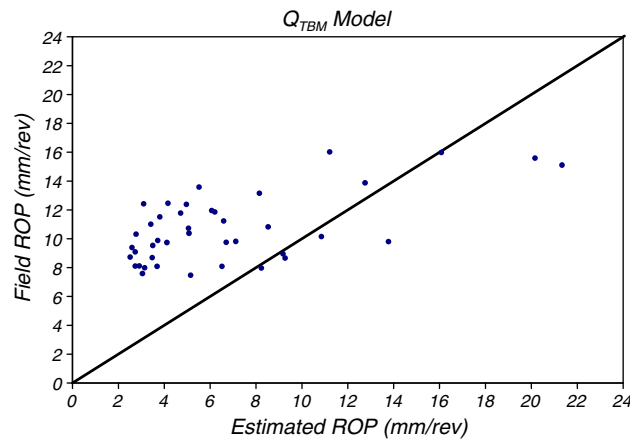
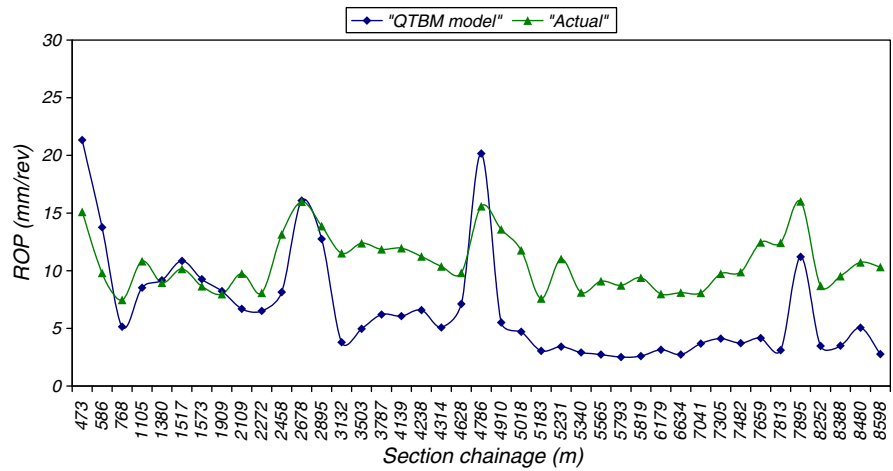
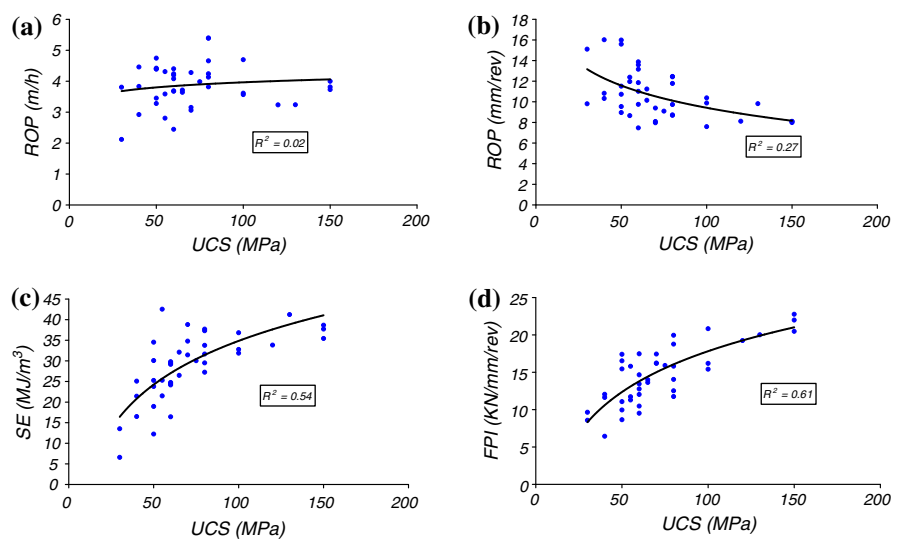


**Fig. 16** Correlation of UCS with TBM parameters **a** ROP (m/h), **b** ROP (mm/rev), **c** SE ( $MJ/m^3$ ) and **d** FPI (KN/cutter/mm/rev)



improving the correlation of RMR with FPI. In fact, water has had an indirect effect on the machine performance with increasing alteration of the rock mass and decreasing strength parameters of the intact rock and joint surface condition.

### 10.5 Rock Mass Strength

In this study, correlation of rock mass strength parameters like  $Q_c$ ,  $\sigma_{cm}$ ,  $UCS_{rm}$  and RMCi with FPI have been investigated (Fig. 20). RMCi which was defined by Eq. 2

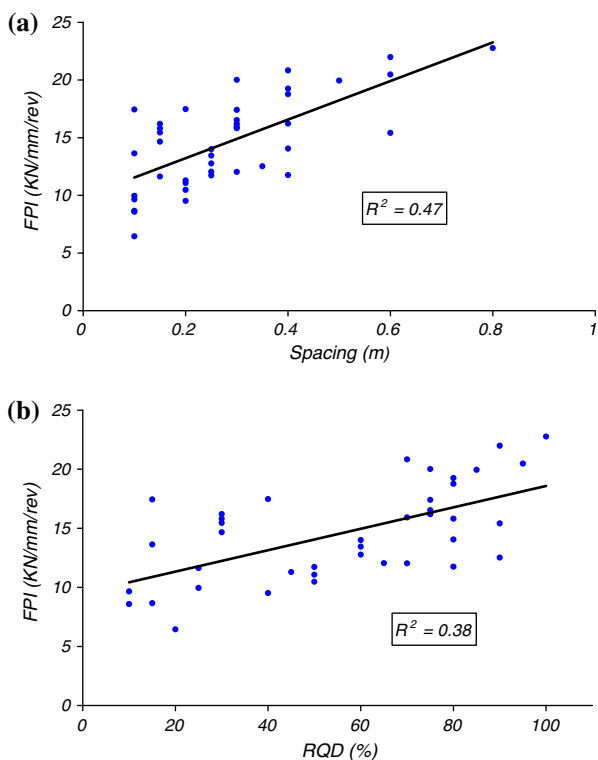


**Fig. 17** Correlation of Spacing (a) and RQD (b) with field penetration index

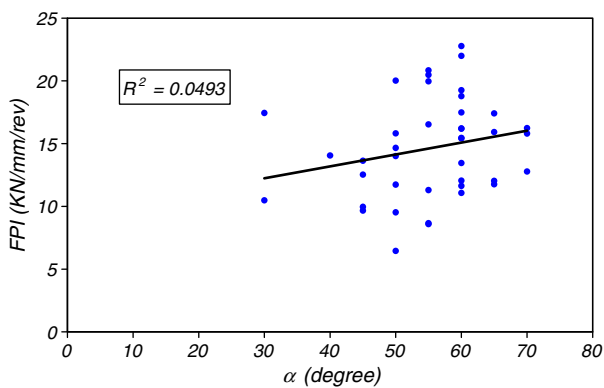


**Fig. 18** Correlation of joint orientation ( $\alpha$ ) with field penetration index

shows the best correlation with FPI. Correlation of  $\sigma_{cm}$  and  $Q_c$  with FPI is very similar to that of  $UCS_{rm}$ .

### 11 Developing New Empirical Equations

In rock engineering practices, statistically based empirical equations have been extensively used to predict a variable based on other operational or geological parameters. Empirical equations have great importance during the early

stages of rock excavation and design works since they are more practical compared to extensive theoretical analyses.

In this study, regression analyses were performed between TBM performance parameters and geomechanical parameters in the database. Both simple regression and multi-variable regression analyses were used to develop empirical equations.

#### 11.1 Simple Regression Analysis

As mentioned in previous sections, among machine parameters, FPI shows the best correlations with geological and geomechanical parameters. Table 8 lists the summary results of correlation of FPI with rock mass parameters and related equations (Eqs. 10 to 20) on a one to one basis.

As shown, among the geomechanical parameters, UCS shows the best correlation with FPI ( $R^2 = 0.612$ ). It seems likely that in Eq. 10 of Table 8, the effect of rock mass fracturing is not considered. In this particular project, there is a relationship between intact rock properties and fracturing condition of the rock mass (usually geological units which include rocks with low values of physical and mechanical properties are more fractured). Actually, values of UCS also reflect the effect of fracturing on TBM performance. So, it can be concluded that the effect of rock mass jointing and fracturing is hidden in Eq. 10.

The RMCI also shows a good correlation with FPI (Eq. 20). This parameter (Eq. 1) is based on two main rock mass parameters, i.e. UCS and RQD (which is an index of fracturing degree of the rock mass). Also FPI (Eq. 8) combines two important machine parameters: rate of penetration or ROP (mm/rev) and net thrust per cutter or  $F_n$  (kN/cutter). All these parameters can be easily determined or estimated, especially in the preliminary stages of the tunnel design and planning. Therefore, it seems likely that Eq. 20 can be a good predictor of the TBM performance in this project and if adjusted for machine specifications, for similar geological conditions.

Ribacchi and Lembo-Fazio (2005) on the basis of data from Varzo tunnel proposed a similar empirical equation which relates  $\sigma_{ca}$  (a parameter similar to  $UCS_{rm}$  in this research) to  $V_{pu}$  (inverse of FPI) as follow:

$$V_{pu} = 250\sigma_{ca}^{-0.667} \tag{21}$$

In Eq. 21,  $V_{pu}$  is penetration rate divided by average cutter thrust or gross thrust/cutter (mm/rev/MN) and  $\sigma_{ca}$  is evaluated on the basis of the correlations between the strength parameter “s” of the Hoek and Brown strength criterion and the quality index of the rock RMR (Hoek et al. 1995). This formula was developed based on the data from a tunnel excavated in a gneiss formation which was characterized by high strength and low fracture intensity, thus the coefficients of equation is a bit different than

**Fig. 19** Correlation of different rock mass classification systems with field penetration index, **a** Basic RMR, **b** RMR<sub>89</sub>, **c** Q-system and **d** GSI

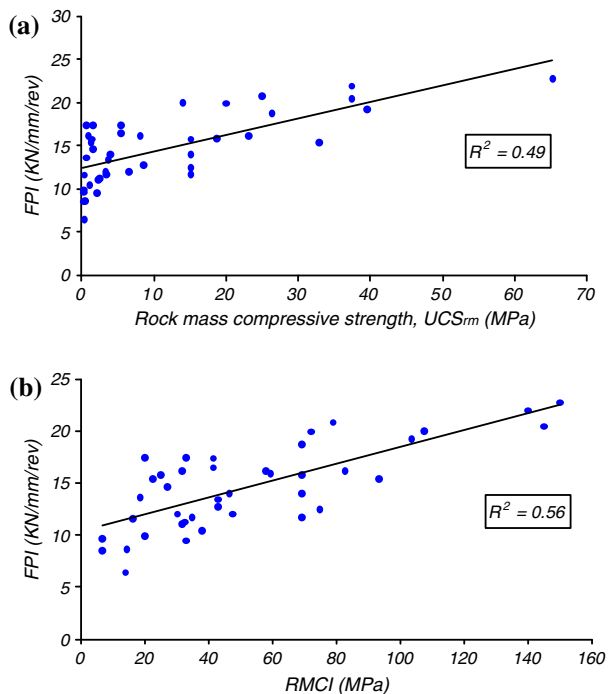
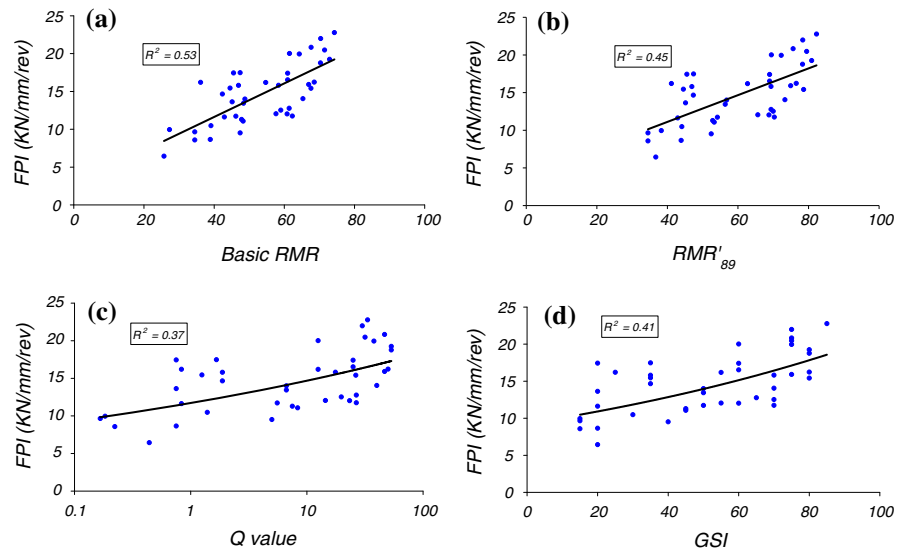


**Fig. 20** Correlation of UCS<sub>rm</sub> (a) and RMCI (b) with field penetration index

Eq. 20. It should be noted that data from Varzo tunnel refer to encountering hard rock with severe problems of boreability.

In this study, an equation similar to Eq. 21 which relates UCS<sub>rm</sub> to FPI is developed (Table 8, Eq. 19). Figure 21 combines two equations in a graph. It should be noted that the equation in Fig. 21 is obtained by replacing FPI and UCS<sub>rm</sub> with  $V_{pu}$  and  $\sigma_{ca}$  in Eq. 19. It is concluded that combining these two projects may lead to a combined

formula for more general applications, if differences in calculating  $\sigma_{ca}$  and UCS<sub>rm</sub> are ignored or reconciled.

## 11.2 Multiple Regression Analysis

In addition to simple regression analyses of different rock mass properties versus TBM parameters, the multiple regression method was also used to find an empirical equation with the best fit with existing data. In this study, the four rock mass properties UCS, joint spacing (or Sp), RQD and  $\alpha$  were input as independent variables and the measured FPI were chosen as a dependent variable. Influence of each variable on the FPI was evaluated using forward stepwise regression analyses. To do these statistical analyses, the SPSS software (a commercial software package for standard statistical analysis, version 11.5, 2002) was used. After checking different combinations of parameters, the variant of excluding the two parameters  $\alpha$  and RQD exhibits the best fit between the parameters Ln(FPI) as response parameter and UCS and  $Sp^{-2}$  as predictors, in a linear combination with a 95% confidence level. As a result, a new performance predictive equation was empirically obtained as follows:

$$FPI = \exp(0.005 UCS - 0.002 Sp^{-2} + 2.338). \quad (22)$$

On the basis of the statistical results, the regression coefficient ( $R^2$ ) is 0.583. It indicates that the above regression model explains 58.3% of the total variance of the 41 datasets.

A simple  $t$  test and  $F$  test analysis of the results indicate that the correlations are real and the coefficients are true.

The measured field penetration index is compared with the predicted one in the selected tunnel sections (Fig. 22). As shown, most of the  $\Delta FPI$  values (difference between

**Table 8** Summary results of determination of regression coefficients of correlation between different geological and geomechanical parameters and FPI

Parameter	Regression coefficient ( $R^2$ )	Regression type	Relationship	Eq. no.
UCS (MPa)	0.612	Logarithmic	$FPI = 7.887 \ln(UCS) - 18.497$	10
Joint frequency				
Spacing (m)	0.472	Linear	$FPI = 16.721 Sp + 9.882$	11
RQD <sub>0</sub> (%)	0.378	Linear	$FPI = 0.091 RQD_0 + 9.528$	12
Rock mass classification systems				
Basic RMR	0.532	Linear	$FPI = 0.222 BRMR + 2.755$	13
RMR' <sub>89</sub>	0.449	Linear	$FPI = 0.178 RMR'_{89} + 4.005$	14
GSI	0.412	Exponential	$FPI = 9.273e^{0.008GSI}$	15
Q	0.369	Power	$FPI = 11.718 Q^{0.098}$	16
Rock mass strength parameters				
Q <sub>c</sub>	0.493	Linear	$FPI = 0.157 Q_c + 12.239$	17
σ <sub>cm</sub> (MPa)	0.494	Polynomial	$FPI = 0.003\sigma_{cm}^2 + 0.016\sigma_{cm} + 11.419$	18
UCS <sub>mm</sub> (MPa)	0.496	Power	$FPI = 11.990 UCS_{mm}^{0.118}$	19
RMCI	0.556	Linear	$FPI = 0.080 RMCI + 10.412$	20

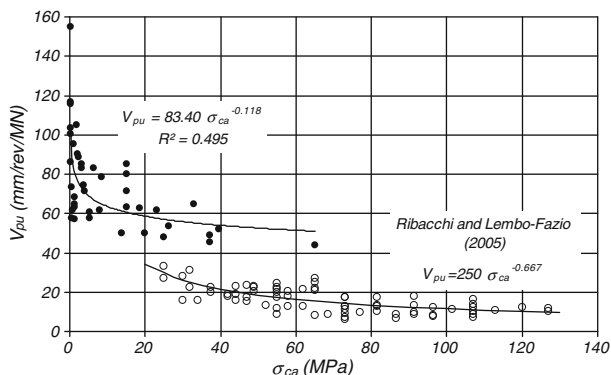


**Fig. 21** Relationship between  $V_{pu}$  and rock mass strength proposed by Ribacchi and Lembo-Fazio (2005) and its combination with Eq. 19

FPI calculated using Eq. 22 and the actual FPI) are less than 4 kN/cutter/mm/rev.

### 11.3 Comparison with Existing Models

As mentioned earlier, results obtained from existing prediction models (CSM, NTNU and  $Q_{TBM}$ ) were compared with actual performance of the machine. Results show that values of ΔROP or difference between penetration rates calculated using various prediction models and the actual penetration rates are very substantially exceeding 100% in some tunnel sections.

Obviously, in a perfect and ideal prediction model absolute values of ΔROP or ΔFPI must be very small. In this section to evaluate accuracy of proposed equations (Eqs. 19, 20 and 22) and compare them with existing prediction models and finally to select the most accurate equation, a descriptive statistical analysis is performed on calculated values of |ΔROP| and |ΔFPI| using SPSS

software. Summary results of descriptive statistical analyses are presented in Table 9 and Fig. 23.

As shown in the Table 9a and b and also in Fig. 23a and b, Eq. 22 with lower mean of computed |ΔROP| and |ΔFPI| values and also lower variance and range of values proves to be the best correlation between rock mass properties and TBM parameters. It is therefore suggested to use Eq. 22 to predict TBM performance in projects with similar geology and machine specification. Obviously more extensive studies of TBM performance in different ground conditions with various machine specifications and operational parameters are required to generalize the results of this study. The reader should bear in mind that the existing models (CSM, NTNU and  $Q_{TBM}$ ) have been developed for general TBM performance and hence should not be expected to have the same accuracy as the equations proposed in this paper, which are specific to this job site and working conditions.

## 12 Conclusions

Based on data obtained from 8.7 km of tunnel in pyroclastic and sedimentary rocks of the Karaj formation, a comparison was made between results of the three most commonly used TBM performance prediction models and actual performance of TBM. The results indicate that the models are applicable in a special range of geological conditions and need some adjustments or correction factors to provide a more accurate estimate of machine performance in certain geological conditions.

In this study, the influence of different geological and geomechanical parameters on the TBM performance was investigated. Analyses revealed that among different

**Fig. 22** Comparison of FPI calculated using the new empirical equation (Eq. 22) with actual FPI

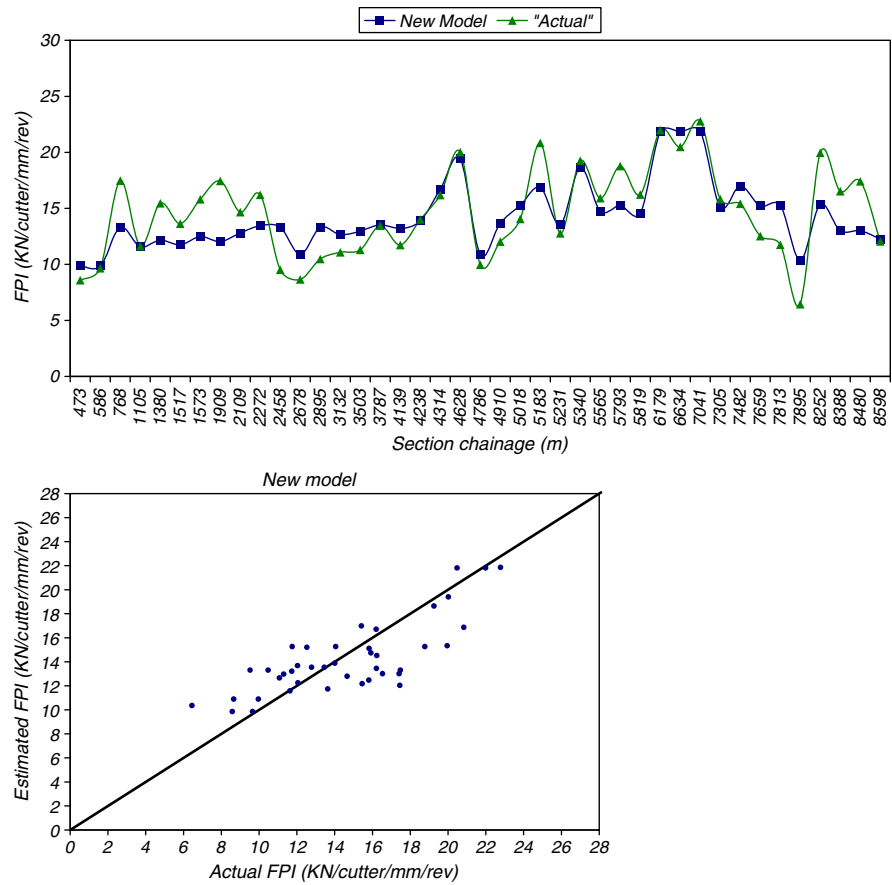


**Table 9** Statistical parameters calculated for  $\Delta$ FPI (a) and  $\Delta$ ROP (b) values obtained from usual prediction models and proposed equations

Statistical parameters	CSM	NTNU	Q <sub>TBM</sub>	Eq. 19	Eq. 20	Eq. 21
<b>(a) <math>\Delta</math>FPII (KN/cutter/mm/rev)</b>						
Mean	11.82	9.18	17.48	2.38	2.19	2.00
Median	4.25	5.24	16.88	2.14	2.05	1.64
Mode	0.08	0.32	0.05	2.10	0.06	0.20
SD	18.33	7.88	14.02	1.43	1.45	1.48
Variance	335.96	62.03	196.65	2.05	2.12	2.18
Range	77.12	25.23	46.37	6.18	5.38	5.36
Minimum	0.08	0.32	0.05	0.07	0.06	0.05
Maximum	77.20	25.55	46.42	6.25	5.44	5.41
<b>(b) <math>\Delta</math>ROPI (mm/rev)</b>						
Mean	3.60	3.45	4.80	1.80	1.76	1.60
Median	3.60	3.40	5.20	1.67	1.62	1.44
Mode	1.30	4.50	6.20	1.47	2.38	1.34
SD	2.30	1.84	2.45	1.25	1.41	1.31
Variance	5.30	3.38	6.01	1.57	1.99	1.72
Range	7.60	7.90	9.20	6.10	7.00	6.00
Minimum	0.10	0.60	0.10	0.06	0.05	0.05
Maximum	7.70	8.50	9.30	6.16	7.05	6.05

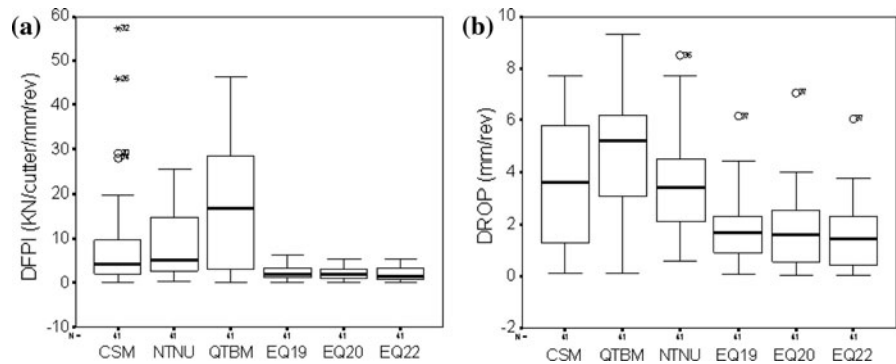
parameters, some composite parameters, such as rock mass cuttability index (RMCI) show better correlation with TBM parameters, especially FPI.

The analyses also indicate that in this particular project intact rock strength has more influence on TBM performance with respect to the fracturing conditions of the rock mass. But this could be due to the close relationship between intact rock properties and fracturing conditions of the rock mass at this site.

Since the proposed equations are based on information of a single tunnel, it is strongly recommended that they are applied with caution and only in similar geological situations, TBM specifications and operating procedure. These equations were developed based on data from layered, moderately to highly jointed detrital sedimentary and pyroclastic rocks with a UCS range of 30 to 150 MPa. They are not recommended in very strong and massive igneous rocks, in very foliated and schistose metamorphic rocks or in very thinly bedded and weak shale or marlstone layers. Clearly, to develop a universal model (or a family of empirical equations) covering different geologies and TBM/operating conditions, it is essential to improve the initial database with collecting more data from different



**Fig. 23** Comparison of  $|\Delta FPI|$  (a) and  $|\Delta ROP|$  (b) values calculated using new empirical equations with  $|\Delta FPI|$  and  $|\Delta ROP|$  values estimated using current models



projects and repeat the analyses to derive new, more general formulas.

**Acknowledgments** Authors wish to thank SCE Company, especially Mr. Gh. Shamsi and his colleagues in the Tunneling Division for their help in the collection of required data. We are also grateful to the reviewers for their careful reading of our manuscript and their many helpful comments.

## References

- Barton N (1999) TBM performance estimation in rock using  $Q_{TBM}$ . *Tunn Tunn Int* 31(9):30–33
- Barton N (2000) TBM tunnelling in jointed and faulted rock. Balkema, Rotterdam, p 173
- Barton N, Lien R, Lunde J (1974) Engineering classification of rock masses for the design of tunnel support. *Rock Mech* 6(4):189–236
- Bieniawski ZT (1989) Engineering rock mass classifications: a complete manual for engineers and geologists in mining, civil and petroleum engineering. Wiley, New York, p 251
- Bilgin N, Kuzu C, Eskikaya S (1997) Cutting performance of rock hammers and roadheaders in Istanbul metro drivages. In: Golser J et al (eds) Proceedings of world tunnel congress 97 and 23rd world assembly of ITA: tunnels for people, Vienna, Austria, Balkema, Rotterdam, pp 455–460
- Blindheim OT (1979) Boreability predictions for tunneling. Ph.D. thesis. Department of geological engineering. The Norwegian Institute of Technology, p 406
- Bruland A (1998) Hard rock tunnel boring: vol 1–10, Ph.D. thesis, Norwegian University of Science and Technology (NTNU), Trondheim, Norway
- Cassinelli F, Cina S, Innaurato N, Mancini R, Sampaolo A (1982) Power consumption and metal wear in tunnel-boring machines: analysis of tunnel-boring operation in hard rock. In: Jones MJ (ed) Tunneling '82, London Institute of Mining Metallurgy, pp 73–81
- Deere DU, Hendron AJ, Patton FD, Cording EJ (1967) Design of surface and near surface construction in rock. In: Fairhurst C (ed) Proceedings of 8th US symposium on rock mechanics. AIME, New York, pp 237–302
- Gong QM, Zhao J (2009) Development of a rock mass characteristics model for TBM penetration rate prediction. *Int J Rock Mech Min Sci* 46(1):8–18
- Hoek E (2007) Rock engineering, Course notes by Evert Hoek. <http://www.Rocscience.com>. p 339
- Hoek E, Kaiser PK, Bawden WF (1995) Support of underground excavations in hard rock. Balkema, Rotterdam, p 215
- Ramezanzadeh A (2005) Performance analysis and development of new models for performance prediction of hard rock TBMs in rock mass. Ph.D. thesis, INSA, Lyon, France, p 333
- Ramezanzadeh A, Rostami J, Tadic D (2008) Impact of rock mass characteristics on hard rock TBM performance. 13th Australian tunneling conference, Melbourne, Australia, pp 213–222
- Ribacchi R, Lembo-Fazio A (2005) Influence of rock mass parameters on the performance of a TBM in a Gneissic formation (Varzo tunnel). *Rock Mech Rock Eng* 38(2):105–127
- Rostami J (1997) Development of a force estimation model for rock fragmentation with disc cutters through theoretical modeling and physical measurement of crushed zone pressure. Ph.D. thesis, Colorado School of Mines, Golden, Colorado, USA, p 249
- Rostami J, Ozdemir L (1993) A new model for performance prediction of hard rock TBM. In: Bowerman LD et al (eds) Proceedings of RETC, Boston, MA, pp 793–809
- Sanio HP (1985) Prediction of the performance of disc cutters in anisotropic rocks. *Int J Rock Mech Min Sci Geomech Abstr* 22(3):153–161
- Sapigni M, Berti M, Behtaz E, Busillo A, Cardone G (2002) TBM performance estimation using rock mass classification. *Int J Rock Mech Min Sci Geomech Abstr* 39:771–788
- SCE Company (2006) Geological and engineering geological reports for KWCT project
- SPSS software (2002) Statistical package, version 11.5. SPSS Inc., Chicago. <http://www.spss.com>
- Yagiz S (2002) Development of rock fracture and brittleness indices to quantify the effects of rock mass features and toughness in the CSM model basic penetration for hard rock tunneling machines. Ph.D. thesis, Department of Mining and Earth Systems Engineering, Colorado School of Mines, Golden, Colorado, USA, p 289
- Yagiz S (2007) Utilizing rock mass properties for predicting TBM performance in hard rock condition. *Tunn Undergr Space Technol* 23(3):326–339